

Time-resolved photoemission at the Si(100)-Ga surface using a femtosecond higher-harmonic laser source

Andrea Melzer, Daniel Kampa, Jinxiong Wang, and Thomas Fauster

Lehrstuhl für Festkörperphysik, Universität Erlangen-Nürnberg, D-91058 Erlangen, Germany

(Received 14 August 2009; revised manuscript received 6 October 2009; published 24 November 2009)

The Si(100)-(2×2)-Ga surface was used to investigate time-dependent Ga(3*d*) core-level shifts by pumping electrons from the valence to the conduction band. The pump-probe experiments were done by exciting carriers with 1.59 eV laser pulses and probing the Ga(3*d*) core level with higher harmonics. The higher harmonics were generated by focusing laser pulses with 1.4 mJ energy, 30 fs pulse duration, and 779 nm wavelength from a multipass amplifier at a repetition rate of 1 kHz into argon. For the 23rd harmonic, the time resolution of the experiment was ~400 fs after a grating monochromator. The band bending of about 110 meV of the *p*-doped Si(100)-(2×2)-Ga surface is completely lifted by illumination of the surface with the 1.59 eV laser pulses. The Ga(3*d*) core level shows a slow time-dependent shift attributed to the rise (~1 ns) and decay (~100 ns) of the photovoltage. The Ga(3*d*) core-level shift and broadening in the femtosecond range are determined to be <15 meV at the used pump-pulse intensity of 19 mJ/cm². Experiments with pump pulses of 3.18 eV photon energy showed similar results.

DOI: 10.1103/PhysRevB.80.205424

PACS number(s): 79.60.Dp, 73.20.-r, 78.47.J-

I. INTRODUCTION

Higher-harmonic generation provides a table-top femtosecond laser source with photon energies in the extended ultraviolet range, enabling time-resolved investigations involving, for example, core-level states. Several applications of time-resolved experiments at surfaces using higher harmonics have already been demonstrated.¹⁻⁸

In this paper, a higher-harmonic photon source is described and used to investigate the charge screening upon laser excitation at the Si(100)-(2×2)-Ga surface. As for the screening of charges upon laser excitation, up to now, no theoretical calculations and also no experimental investigations exist; the study of this effect is of fundamental physical interest.

To observe a change in screening upon laser illumination, high excitation densities are necessary. So silicon was chosen as substrate for the experiments, as it has long carrier lifetimes being an indirect semiconductor. Gallium was chosen as adsorbate, as it has a relative shallow 3*d* core level with a binding energy of about 19 eV. The chosen Si(100)-(2×2)-Ga surface has a semiconducting surface,^{9,10} enabling high excitation densities.

Figure 1 illustrates the concept of the measurement. In thermal equilibrium, the bands at the surface are bent downward for a *p*-doped Si substrate. The adsorbed Ga provides a shallow 3*d* core level as well as occupied and unoccupied surface states. Upon excitation with infrared (or visible) light the excitation of electrons from the valence band (VB) to the conduction band (CB) reduces the band bending. For sufficiently high intensities, a flat band condition is reached and the resulting photovoltage U_{PV} corresponds to the initial band bending. In a photoemission experiment, the energies are measured relative to the bulk Fermi level E_F , and the illumination shifts all energy levels by an amount corresponding to the photovoltage. The additional shift in the Ga(3*d*) core level can be measured using the higher-harmonic pulses. The measured binding energy corresponds

to the core hole screened by the surrounding electrons. The light pulse can also excite carriers from the occupied to the unoccupied Ga surface state. The changed carrier distribution should lead to an additional change in screening and thus to a different kinetic energy of the photoelectrons ionized by the higher harmonics. The time evolution of the screening charge can be detected in a pump-probe experiment.

II. EXPERIMENTAL SETUP

The experimental setup (see Fig. 2) consists of a femtosecond Ti:sapphire amplifier system, the vacuum chamber for generating the higher harmonics, the monochromator chamber and the ultrahigh-vacuum (UHV) chamber for sample preparation and examination.

A. Laser system

The Ti:sapphire multipass amplifier delivers laser pulses with 1.4 mJ pulse energy, 30 fs pulse duration, and 779 nm

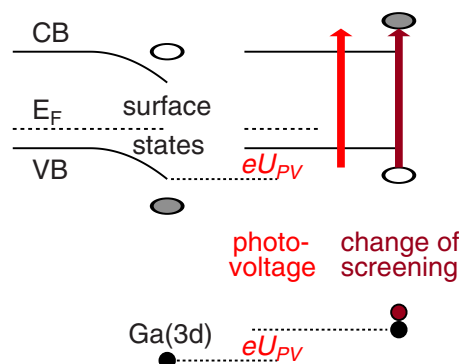


FIG. 1. (Color online) Schematic energy diagram of the Si(100)-(2×2)-Ga surface with unoccupied and occupied surface states. The band bending (left panel) is lifted by illumination with light leading to a photovoltage (right panel). The energy of the Ga(3*d*) hole might experience an additional shift due to the change in the screening after excitation of electrons from occupied to unoccupied surface states.

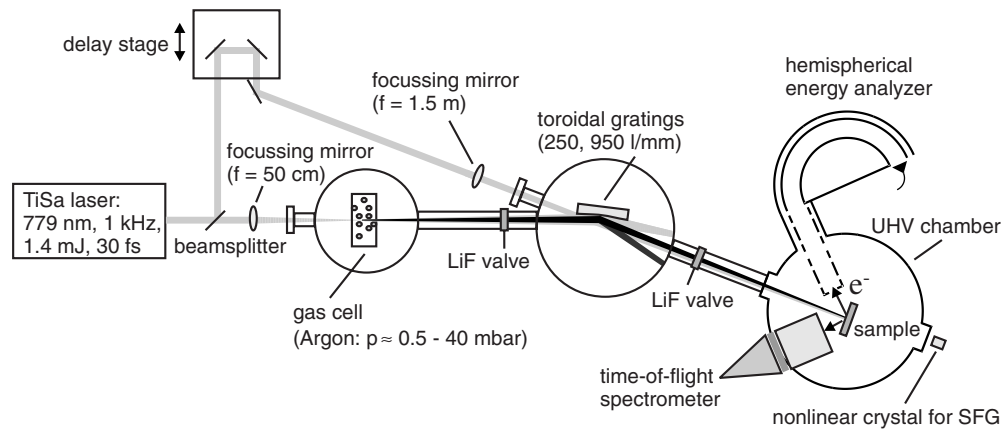


FIG. 2. Layout of the experimental setup.

wavelength at a repetition rate of 1 kHz. The design and performance of the amplifier system is described in Ref. 11. 90% of the output power of the amplifier are used to generate the higher harmonics, the other 10% are used as pump pulses for the time-resolved experiments.

The higher harmonics are generated by focusing the amplified laser pulses by a mirror with 50 cm focal length into a gas cell filled with argon. As gas cell, a squeezed stainless steel tube is used, in which the laser itself drills a hole to minimize the gas flow to the surrounding vacuum chamber.¹² The gas target length was 2–3 mm and backing pressures up to 40 mbar are used. To reduce the gas flow to the UHV chamber, the vacuum chamber housing the gas cell is differentially pumped and the diameter of the tubes between the different vacuum chambers are chosen as small as possible according to the respective beam diameter. At the highest backing pressures used in the gas cell of 40 mbar, the pressure in the UHV chamber rose from $<3 \cdot 10^{-11}$ to $\sim 1 \cdot 10^{-10}$ mbar. To select an individual harmonic, two toroidal gratings in the monochromator chamber can be used with 250 and 950 lines/mm, optimized for different energy ranges.¹³ The selected harmonic is focused by the grating onto the sample. For time-resolved measurements the 1.59 eV pump pulses, are focused onto the sample by a mirror of 1.5 m focal length. To determine the spatial overlap of the infrared (IR) and the harmonic pulses a fluorescence screen can be placed at the position of the sample. To determine the temporal overlap, a beta barium borate (BBO) crystal is placed behind the sample outside the UHV chamber. Turning the grating to the zeroth order, the IR light is transmitted, and the sum frequency signal generated in the BBO crystal of this beam and the IR pump beam determines the temporal overlap at the position of the BBO crystal. The temporal overlap at the sample position can then be calculated. Between the vacuum chambers valves with LiF windows are placed. These valves are kept closed when using the third or fifth harmonic in order to eliminate the background signal due to higher harmonics diffracted in higher order.

B. Energy analyzers

For the photoemission experiments, a hemispherical energy analyzer and a time-of-flight spectrometer can be used

in the UHV chamber for electron detection. The hemispherical energy analyzer has an energy resolution of 35 meV at 2 eV pass energy and an angular resolution of $\pm 1^\circ$. The time-of-flight spectrometer was designed with a large detection angle of $\pm 17^\circ$ to achieve a high detection efficiency for non-dispersing core levels. Alternatively, an anode segment with a detection angle of $\pm 2^\circ$ can be chosen, if good angular resolution is desired. The electrons pass a field free flight distance of about 213 mm and are detected by a chevron pair of microchannel plates with 120 mm diameter. The amplified signal then passes a discriminator and is fed to a picosecond time analyzer,¹⁴ which measures the arrival time of the electrons. The start pulse is derived from the Pockels cell driver of the laser system or a fast photodiode. The time resolution of the spectrometer was measured as 300 ps, corresponding to an energy resolution of 18 meV for electrons with 5 eV kinetic energy and 146 meV for electrons with 20 eV kinetic energy.

The sensitivity of both electron analyzers normalized to the same energy interval and angular acceptance is comparable. The time-of-flight spectrometer has a big advantage, if a large acceptance angle can be used and wide energy spectra are of interest. In this paper, only the data of Sec. VII were taken with the time-of-flight spectrometer. For all other measurements, the hemispherical analyzer was used. All photoelectron spectra were taken in normal emission.

C. Characterization of higher harmonics

For characterization of the experimental setup Cu(111) and Pd(111) surfaces were used. Photoemission spectra with higher harmonics up to the 33rd order (52 eV) can be recorded with the hemispherical energy analyzer and up to the 39th order (62 eV) with the time-of-flight spectrometer. The linewidths of the harmonics could be determined by evaluation of the measured linewidths of the occupied Shockley surface state¹⁵ of the Cu(111) surface. The linewidths increase approximately linearly from about 110 meV for the fifth harmonic (7.8 eV) to 790 meV for the 29th harmonic (47 eV) in qualitative agreement with previous reports.¹⁶ The increase is due to the decreasing resolution of the grating monochromator and the increase in linewidth with the har-

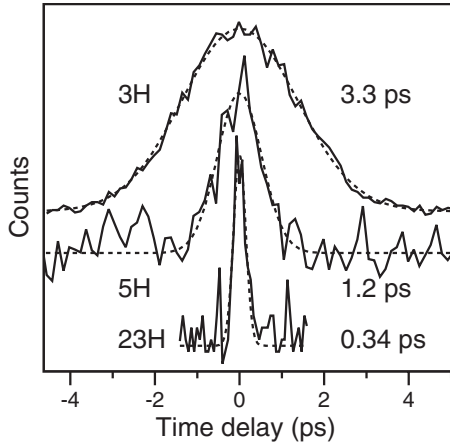


FIG. 3. Time-resolved measurements for the unoccupied surface state on Pd(111) using IR pump pulses and the third, fifth, and 23rd harmonic (4.8, 7.8, and 37 eV photon energy) as probe pulses. The spectra are normalized to the same maximum above the baseline, which is offset for clarity. Dashed lines show fits using a Gaussian function.

monic order.¹⁷ The latter contribution depends strongly on laser parameters, so a quantitative comparison is not possible.

The pulse durations of the harmonics directly after the generation process are expected to be ≤ 30 fs. By diffraction at the grating, the harmonics are temporally broadened. For a flat grating, the path difference for laser rays diffracted at different positions at the grating leads to a temporal broadening of $\Delta t \propto N \cdot \lambda / c$ for diffraction in the first grating order, where N is the number of illuminated grating grooves. The dependence on N can be checked by using the third harmonic in positive and negative order, which leads to an illumination of the grating differing by a factor of two. The cross correlation with the IR pulse measured for the image-potential state on Cu(111) (Ref. 18) varies indeed by the same factor. The pulse duration should vary proportional to the wavelength and thus indirectly proportional to the harmonic order. Figure 3 shows measurements for the third, fifth, and 23rd harmonic using the two-photon signal of the unoccupied Shockley surface state¹⁹ of the Pd(111) surface. The surface state is excited with the IR pulses and ionized with the harmonics. Fits using a Gaussian function yield values for the pulse duration of 3.3 ± 0.2 , 1.2 ± 0.1 , and 0.34 ± 0.03 ps, respectively. The expected dependence inversely proportional to the harmonic order is found within the error bars. Note that the data in Fig. 3 are scaled to maximum intensity above the baseline. In particular, for the fifth harmonic, the background intensity due to one-photon photoemission is rather large leading to a poor statistics. For the seventh and higher harmonics, the pulse duration and thus, the time resolution of the experiment is in the femtosecond range. The proportionality factor in the equation for Δt depends on the beam profile and the shape of the toroidal grating. It could be estimated using ray-tracing methods. The beam profile of the higher harmonics is not easily accessible in experiment and known to be narrower than that of the IR beam.²⁰

III. Si(100)-(2×2)-Ga SURFACE

The Si(100)-(2×2)-Ga surface is obtained by evaporating half a monolayer of Gallium onto the clean Si(100)-(2×1)-surface. The Si(100)-Ga surface shows a (2×2) low-energy electron diffraction (LEED) pattern at coverages from 0.40–0.55 monolayers.²¹

At the coverage of half a monolayer, all the dangling bonds of the Si(100)-(2×1)-surface are saturated. Each Gallium atom forms two Ga–Si bonds and one Ga–Ga bond. The Ga dimers are aligned parallel to the underlying Si dimers forming Ga dimer rows perpendicular to the Si dimer rows. Details of the geometric structure of the Si(100)-(2×2)-Ga surface can be found in Refs. 22 and 23. As the Ga atoms are sp^3 -like hybridized, one empty sp^3 orbital is remaining at each Ga atom, forming an unoccupied surface state, which can be imaged by scanning tunneling microscopy.^{10,24} The electronic structure of the occupied surface bands was investigated in Ref. 9 by angle-resolved photoemission and interpreted further in Ref. 25, showing 5 occupied bands at energies of 1–2 eV below the Fermi energy. The unoccupied surface state was observed by scanning tunneling spectroscopy 1.44 eV above the Fermi energy.¹⁰

Si(100) samples were cut from p -doped wafers (B, 7–13 Ωcm) and the sample preparation followed the procedures described in Refs. 26 and 27. The clean Si(100)-(2×1)-surface always showed a sharp (2×1) LEED pattern at room temperature. The preparation of the Si(100)-(2×2)-Ga-surface followed the procedures described before.^{9,21,28} Half a monolayer Gallium was evaporated from an alumina crucible, followed by annealing the sample at 390 °C for 10 min. A sharp (2×2) LEED pattern was observed, if the evaporation time was chosen correctly. All measurements were done at room temperature.

IV. SURFACE STATES

As described in the introduction, an excitation of carriers into the unoccupied Ga surface state could lead to a very effective screening of Ga(3d) core holes. To clarify this possibility, one-photon photoemission spectra with the higher harmonics and two-photon photoemission spectra with the third harmonic and the IR light were recorded. The IR power was typically 2 mW in order to ensure saturation of photovoltage and limit multiphoton photoemission background (see Sec. V).

Figure 4 shows a one-photon photoemission spectrum recorded with the fifth harmonic [the spectrum is corrected for the band bending (see Sec. V)] and three two-photon photoemission spectra recorded with the third harmonic and the IR light for different time delays. The spectrum of the fifth harmonic shows a peak 1.0 eV below the Fermi energy. The two-photon spectrum at nearly zero time delay (dashed line) clearly shows a peak 0.8 eV above the Fermi energy, which is assigned to the unoccupied Ga surface state. The surface state is excited by the IR light and ionized with the third harmonic, as the time dependence of the peak intensity shows (see also Fig. 5). For negative time delays (third harmonic first) no peak is visible (dotted line) and for positive time delays the intensity of the peak decreases according to

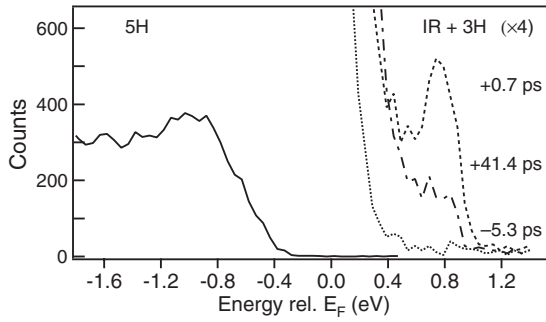


FIG. 4. One-photon photoemission spectrum of the Si(100)-(2 × 2)-Ga surface, recorded with the fifth harmonic (7.8 eV) and two-photon photoemission spectra for different time delays of the third harmonic (4.8 eV) and the IR light. An occupied state is observed 1.0 eV below the Fermi energy and the unoccupied state 0.8 eV above the Fermi energy.

the lifetime of the state. For a positive time delay of ~40 ps (dash-dotted line) the intensity of the peak has decreased significantly. The remaining intensity is mainly due to a slowly decaying background always observed between the Fermi energy and an energy of ~0.95 eV above the Fermi energy. The background might be attributed to the occupation of defect states in the band gap, which have at the clean Si(100) surface lifetimes in the ns range.²⁷ For energies above $E_F + 0.88$ eV, electrons excited into the bulk conduction band might play a role that show time scales of 200 ps.^{29,30} Fig. 5 presents time-resolved measurements for the unoccupied surface state at $E_F + 0.8$ eV. The data can be fitted by a biexponential decay with lifetimes of 2.7 ± 0.5 ps and ≈ 150 ps. The latter value matches quite well with the time scale for electrons excited into the bulk conduction band that are subsequently scattered into surface states.³⁰ The shorter value is assigned to the lifetime of the unoccupied Ga surface state. Similar values are observed for the unoccupied surface state on the clean Si(100) surface.²⁹

The measured energy of the unoccupied Ga surface state is considerably lower than the energy of 1.44 eV above E_F from the measurements in Ref. 10. This can partly be due to a different sample doping. Furthermore the field of the scanning tip can introduce a band bending at the surface, leading

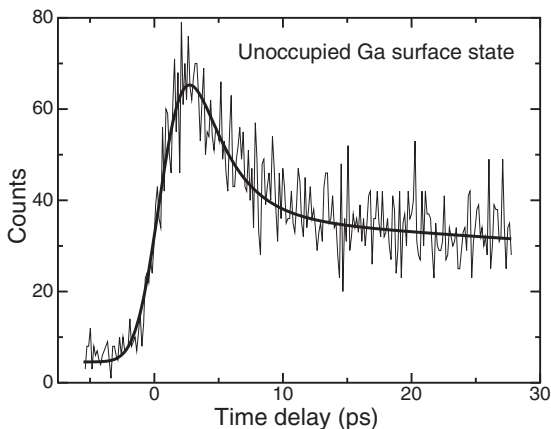


FIG. 5. Time-resolved measurement with the third harmonic and the IR light for the unoccupied Ga surface state 0.8 eV above E_F .

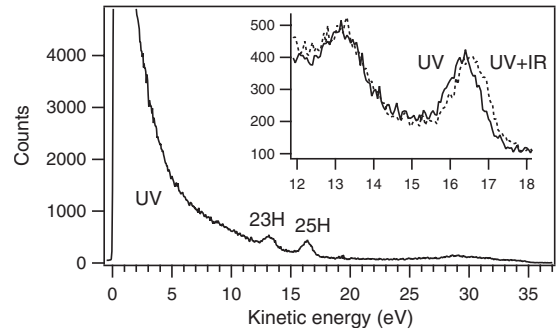


FIG. 6. Photoelectron spectrum from the Si(100)-(2 × 2)-Ga surface excited with the 23rd and 25th harmonic (37 and 40 eV photon energy). The inset shows the Ga(3d) lines on an enlarged scale. Data taken with IR light overlapping with the 25th harmonic only are plotted as a dashed curve and exhibit a shift due to the photovoltage created by the IR light.

to an energy shift in unoccupied states to higher energies, which was observed for similar conditions in Ref. 31. The measured energy of the occupied surface state is consistent with the previous photoemission results taking into account that no information on the band bending and the position of the Fermi energy with respect to the valence band maximum is given in Ref. 9.

The measurements in Fig. 4 show, that at the used photon energy of 1.59 eV an excitation into the unoccupied Ga surface state is possible and at a photon energy of 1.8 eV a resonant excitation would be possible. The measurements are supported by reflectance anisotropy measurements of Ref. 32, where also a resonance at 1.8 eV was observed.

V. BAND BENDING AND PHOTOVOLTAGE

Semiconductor surfaces generally show a band bending at the surface. By illumination with photons of an energy larger than the band gap, electron-hole pairs are created, which separate in the electric field of the space-charge layer and lead to a compensation of the band bending, denoted as photovoltage (see Fig. 1). As the band bending causes an energetic shift in the electron states at the surface, it is necessary to know the value of the band bending or to have flat bands, to be able to refer the measured energies to the valence band maximum in the bulk.

Figure 6 shows a photoelectron spectrum taken with the 23rd and 25th harmonic illuminating the sample at different points observed simultaneously by the spectrometer. The low-energy cutoff is dominated by secondary electrons emitted from the vacuum level of the sample. The valence band at high kinetic energies is smeared out because of the use of two-photon energies separated by 3.2 eV. The Ga(3d) lines appear also twice at kinetic energies around 13 and 16 eV. Due to the bandwidth of the laser pulses and the chosen analyzer resolution the $3d_{3/2}$ and $3d_{5/2}$ doublet is not resolved.

The inset of Fig. 6 shows the Ga(3d) lines on an enlarged scale. The dashed curve was measured with the IR light overlapped with the 25th harmonic. Only the peak excited with the 25th harmonic is shifted by the simultaneous illumination

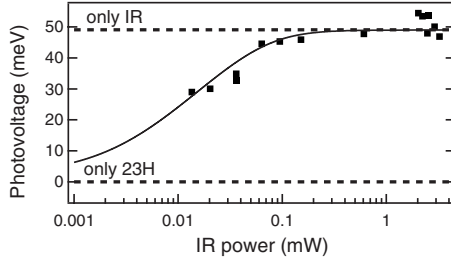


FIG. 7. Measured IR-power dependence of the photovoltage. The photovoltage was determined by evaluating the low-energy cutoff of spectra recorded with the 23rd harmonic and different power of the IR light. The 23rd harmonic causes no photovoltage (lower dashed line). The photovoltage is saturated (upper dashed line) at IR-power levels < 3 mW before the multiphoton photoemission is observed. The solid line shows a fit using the model of Mönch (Ref. 35).

with the IR light. This proves that the photovoltage is caused by the IR light.

As p -doped samples are used the bands at the Si(100)-(2 \times 2)-Ga surface are shifted to lower energies. The band gap of silicon is 1.12 eV at room temperature and the valence band maximum at room temperature is 0.24 eV below the Fermi energy as calculated from doping. Illumination with the higher harmonics causes no photovoltage at the Si(100)-(2 \times 2)-Ga surface, as was seen from measurements with different intensities of the harmonics. By illumination with the intense IR pulses, the band bending is completely lifted at IR power larger 0.5 mW (see Fig. 7), leading to a saturated photovoltage and flat bands. For the data of the photovoltage as function of IR power shown in Fig. 7 the low-energy cutoff of spectra recorded with the 23rd harmonic was evaluated. The zero level of the photovoltage in Fig. 7 is set to the low-energy cutoff of spectra measured with the 23rd harmonic only (lower dashed line). The IR light causes multiphoton photoemission processes^{33,34} at intensities larger ~ 3 mW. The low-energy cutoff of this multiphoton background coincides with the saturated photovoltage (upper dashed line). As the harmonics cause no photovoltage the saturated photovoltage corresponds to the initial band bending of the sample. From measurements for different sample preparations, we obtain a mean value of 110 ± 48 meV for the band bending of the Si(100)-(2 \times 2)-Ga surface.

The intensity dependence of the photovoltage can be described by a model of Mönch,³⁵ yielding following relation between the laser power P and the photovoltage $U_{PV}(P) = u_{PV}(P) \cdot k_B T / e$:

$$\frac{e^{u_{PV}(P)} - 1}{\sqrt{u_{BB} - u_{PV}(P)}} = c \cdot P. \quad (1)$$

$U_{BB} = u_{BB} \cdot k_B T / e$ here is the band bending without laser illumination and c is a constant, which can be calculated from experimental parameters:

$$c = \frac{4}{A_R^* \pi R^2 \hbar \omega} \sqrt{\frac{\epsilon_r \epsilon_0 k_B}{N_A T^3}} e^{u_{BB}}. \quad (2)$$

Here, $A_R^* = e k_B^2 m^* / (2 \pi^2 \hbar^3)$ is the effective Richardson constant, m^* the effective mass of the majority carriers, α the

absorption coefficient, and R the laser beam radius at the sample. With the known values of the parameters, the constant c is calculated as $1.3 \cdot 10^{-5} \text{ W}^{-1}$.

The constant c can also be determined from a fit of Eq. (1) to the measured intensity dependence of the photovoltage. The fit is shown in Fig. 7 as solid line and yields a value of $c = 0.7 \cdot 10^{-5} \text{ W}^{-1}$, in quite good agreement with the calculated value. The difference of the two values can be attributed to uncertainties of the experimental parameters.

VI. TIME DEPENDENCE OF THE PHOTOVOLTAGE

The rise of the photovoltage takes place on a time scale < 1 ps, as was shown in Ref. 36 by reflective electro-optic sampling measurements at a GaAs(100) surface and by theoretical calculations. In photovoltage measurements using photoemission spectra, care in interpreting the results must be taken as macroscopic effects influence the measurement. The build-up of the photovoltage causes a sudden potential change in the illuminated sample area. This macroscopic potential influences electrons on a macroscopic length scale, that means it influences also electrons that have left the surface before the photovoltage is built up. The magnitude of the potential change transferred to the electrons depends on their distance from the surface. This effect may lead to a clearly slow rise of the photovoltage in time-resolved photoemission experiments.^{37,38} As electrons with higher kinetic energy move faster away from the surface, they experience a larger potential change than slower electrons emitted at the same time and thus, a faster rise time of the photovoltage is measured. The decay of the photovoltage for the used surface is expected to take place on a ns-time scale. For similar surfaces, as, for example, the SiO₂/Si(100) surface, decay times in the range of 100 ns were found.^{37,39}

To determine the time dependence of the photovoltage on the Si(100)-(2 \times 2)-Ga surface, spectra of the Ga(3d) core-level state with the 25th harmonic and the IR light for different time delays on a ps-time scale were recorded, and for each spectrum the position of the Ga(3d) peak was evaluated. The Ga(3d) peak and not the low-energy cutoff was used, because the rise of the photovoltage takes place on a shorter time scale for electrons with higher kinetic energy and can thus be better observed with our setup.

The obtained time dependence of the photovoltage for a pump power of 20 mW is shown in Fig. 8. The zero point of the photovoltage is obtained from spectra measured with the 25th harmonic alone. For positive time delays (IR first) up to 100 ps, no change in the photovoltage is observed, in agreement with the expected decay time on a time scale of ~ 100 ns. For negative time delays, due to the above described macroscopic effects, also a photovoltage is measured. The increase in the photovoltage takes place on time scale of ~ 1 ns. In Ref. 37, an increase in the photovoltage on a time scale of ~ 400 ps on a SiO₂/Si(100) surface was measured. In this reference, an analytical model for the shape of the potential in front of the sample is given, whereby the potential shape depends only on the laser beam radius at the sample and the distance of the electrons from the sample at the time of the photovoltage build-up. The distance of the

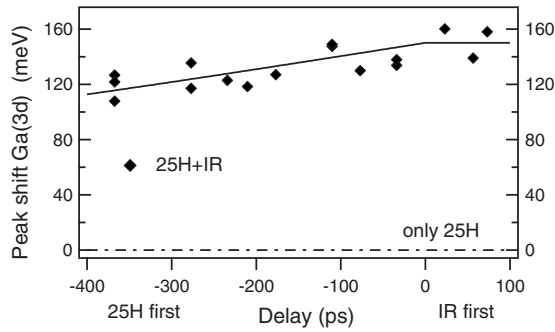


FIG. 8. Time dependence of the photovoltage, obtained by evaluation of the Ga(3d) peak position of spectra recorded for different time delays of the 25th harmonic and the IR light.

electrons can be converted into a time, from which the temporal evolution of the photovoltage is derived. This model could explain the results of Ref. 37. Using this model to fit the data of Fig. 8 gives a beam radius of 3.7 mm, about 16 times larger than the real beam radius of 225 μm . The reason for this discrepancy is not known. A residual photovoltage of the previous laser pulse can be excluded, as the pulse separation is 1 ms and the photovoltage has fully decayed after this time. A residual photovoltage of a prepulse can also be excluded. The prepulse of the Pockels cell was suppressed for the measurement and the parasitic prepulse, that hits the sample 6.8 ns before the main pulse, has a more than 10^3 times smaller intensity than the main pulse.¹¹

For GaAs(100), much shorter time scales have been observed using Ga 3d core-level shifts.⁴ These time scales were confirmed by two-photon photoemission experiments.⁴⁰ The short time scales for the rise and fall time of the photovoltage can be attributed to a much faster recombination of surface and bulk carriers for GaAs.

VII. INVESTIGATION OF THE CHARGE SCREENING

A change in charge screening upon laser excitation should take place on a femtosecond time scale. If the screening of the Ga(3d) core hole is dominated by the Ga surface states, core-level shifts should be observable for a few picoseconds after excitation by an IR pulse (see Sec. IV and Fig. 5). As the photovoltage shows a time dependence on a time scale of several 100 ps (see Fig. 8), it can be considered as constant on a femtosecond time scale. The macroscopic effects leading to the slow dynamics of the photovoltage do not occur for the local screening, which is almost immediate.

To investigate the charge screening upon laser excitation, spectra of the Ga(3d) core level with the harmonics (23rd–29th) and the IR light for different time delays on a femtosecond time scale were recorded. To reduce the multiphoton background, the IR pulses were temporally stretched to about 250 fs by letting the IR beam traverse 11 cm of water. The time resolution of the experiment of ~ 400 fs results from the pulse duration of the harmonics and the IR light. The pump power of the IR light was 10 mW. For each time delay, the first and the second moment of the Ga(3d) peak was evaluated as measure of the energetic position and

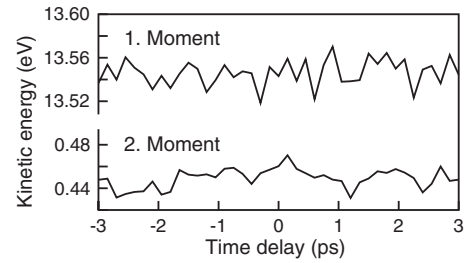


FIG. 9. Energy (first moment) and width (second moment) of the Ga(3d) peak as a function of time delay between the 23rd harmonic and the IR light.

width. The results are shown in Fig. 9. From the measurements, only an upper limit for the Ga(3d) core-level shift and broadening of 15 meV at the highest used IR intensity of 19 mJ/cm^2 could be determined. At higher IR intensities, a measurement was not possible as the multiphoton background causes a disturbing background signal at the position of the Ga(3d) peak. Furthermore, the IR multiphoton background causes space-charge effects,^{41,42} leading to a shift and broadening of the Ga(3d) peak. To obtain a higher carrier excitation, experiments using the second harmonic instead of the IR light as pump pulse were performed, but no significant effect was observed as well.

The failure to observe significant core-level shifts induced by changing the screening charge can have different reasons. (i) The effect is too small to be detected experimentally. As for the investigated effect, no quantitative theoretical calculations exist, its size is not known. However, the effect may be larger for other surfaces. Therefore, in future measurements, the investigation of another system would be reasonable. For example, germanium on Si(100) could be used, as germanium has a core-level state with a binding energy of ~ 30 eV, which can be probed with the higher harmonics. (ii) The screening of the core hole is dominated by all valence electrons around the Ga atom and the contribution from the surface states is negligible. (iii) Not enough carriers were excited to induce a detectable change in screening. A higher excitation density could on the one hand be obtained by using an optical-parametric amplifier, allowing a resonant excitation on the Si(100)-(2 \times 2)-Ga surface at 1.8 eV into the unoccupied Ga surface state (see Sec. IV). On the other hand, the pump-pulse intensity would have to be increased. Higher pump-pulse intensities in principle are available, but due to the multiphoton background in the spectra, these could not be used. For detecting the Ga(3d) core-level state at energies above the multiphoton background at larger pump-pulse intensities, the use of higher photon energies would be necessary.

VIII. SUMMARY AND CONCLUSIONS

We have presented an investigation of time-dependent Ga(3d) core-level shifts on the Si(100)-(2 \times 2)-Ga surface using a higher-harmonic photon source in combination with 1.59 and 3.18 eV pump pulses. The band bending of the Si(100)-(2 \times 2)-Ga surface of 110 ± 48 meV can be completely lifted by illumination with intense IR pulses. The

induced photovoltage shows a time dependence with an onset on a time scale of about 1 ns and a decay on a much longer time scale. The measured rise time is much slower than the expected build-up of the photovoltage on a time scale of <1 ps, which can be explained by the macroscopic potential change in the sample linked to the photovoltage build-up. Due to the time dependence on a time scale of several 100 ps, the photovoltage can be considered as constant on the expected fs time scale of the core-level screening. As result of the study of the Ga(3d) core-level screening upon laser excitation on a fs time scale, only an upper limit for the Ga(3d) core-level shift and broadening of 15 meV could be determined. Using the second harmonic instead of the IR light for carrier excitation, no significant effect was observed as well. Different reasons for the absence of significant core-level shifts induced by changing the screening were discussed.

Pump-probe experiments using a higher-harmonic source rely on a strong IR pump pulse because the weak higher harmonics can serve only as probe pulses. The main problem is the multiphoton photoemission background created by the pump light, which restricts the achievable excitation densities. This fundamental limitation can be alleviated by the use of higher photon energies for the probe pulse. This shifts the photoelectron peaks away from the multiphoton photoemission background toward higher kinetic energies at the expense of a decrease in energy resolution.

ACKNOWLEDGMENTS

We thank M. Kutschera, I. L. Shumay, M. Weinelt, M. Wiets, and A. Wulff for various contributions during the development of the experimental setup. We appreciate the help of K. Biedermann with fitting the time-resolved data.

-
- ¹R. Haight, Surf. Sci. Rep. **21**, 275 (1995).
²F. Quéré, S. Guizard, Ph. Martin, G. Petite, H. Merdji, B. Carré, J.-F. Hergott, and L. Le Déroff, Phys. Rev. B **61**, 9883 (2000).
³M. Bauer, C. Lei, K. Read, R. Tobey, J. Gland, M. M. Murnane, and H. C. Kapteyn, Phys. Rev. Lett. **87**, 025501 (2001).
⁴P. Siffalovic, M. Drescher, and U. Heinzmann, Europhys. Lett. **60**, 924 (2002).
⁵L. Miaja-Avila, C. Lei, M. Aeschlimann, J. L. Gland, M. M. Murnane, H. C. Kapteyn, and G. Saathoff, Phys. Rev. Lett. **97**, 113604 (2006).
⁶A. L. Cavalieri, N. Müller, T. Uphues, V. S. Yakovlev, A. Baltuška, B. Horvath, B. Schmidt, L. Blümel, R. Holzwarth, S. Hendel, M. Drescher, U. Kleineberg, P. M. Echenique, R. Kienberger, F. Krausz, and U. Heinzmann, Nature (London) **449**, 1029 (2007).
⁷S. Mathias, M. Wiesenmayer, F. Deicke, A. Ruffing, L. Miaja-Avila, M. M. Murnane, H. C. Kapteyn, M. Bauer, and M. Aeschlimann, J. Phys.: Conf. Ser. **148**, 012042 (2009).
⁸T. Haarlammert and H. Zacharias, Curr. Opin. Solid State Mater. Sci. **13**, 13 (2009).
⁹Y. Enta, S. Suzuki, and S. Kono, Surf. Sci. **242**, 277 (1991).
¹⁰H. Sakama, A. Kawazu, T. Sueyoshi, T. Sato, and M. Iwatsuki, Phys. Rev. B **54**, 8756 (1996).
¹¹J. Wang, M. Weinelt, and T. Fauster, Appl. Phys. B: Lasers Opt. **82**, 571 (2006).
¹²M. Schnürer, Ch. Spielmann, P. Wobrowschek, C. Strelt, N. H. Burnett, C. Kan, K. Ferencz, R. Koppitsch, Z. Cheng, T. Brabec, and F. Krausz, Phys. Rev. Lett. **80**, 3236 (1998).
¹³Jobin-Ivon I.S.A., # 540 00 810 and # 540 00 800.
¹⁴Ortec, 9306, 9307, 9308-PCI.
¹⁵P. O. Gartland and B. J. Slagsvold, Phys. Rev. B **12**, 4047 (1975).
¹⁶G. Tsilimis, C. Benesch, J. Kutzner, and H. Zacharias, J. Opt. Soc. Am. B **20**, 246 (2003).
¹⁷P. Villoresi, P. Barbiero, L. Poletto, M. Nisoli, G. Cerullo, E. Priori, S. Stagira, C. De Lisio, R. Bruzzese, and C. Altucci, Laser Part. Beams **19**, 41 (2001).
¹⁸T. Hertel, E. Knoesel, M. Wolf, and G. Ertl, Phys. Rev. Lett. **76**, 535 (1996).
¹⁹A. Schäfer, I. L. Shumay, M. Wiets, M. Weinelt, Th. Fauster, E. V. Chulkov, V. M. Silkin, and P. M. Echenique, Phys. Rev. B **61**, 13159 (2000).
²⁰P. Salières, T. Ditmire, M. D. Perry, A. L'Huillier, and M. Lewenstein, J. Phys. B **29**, 4771 (1996).
²¹B. Bourguignon, K. L. Carleton, and S. R. Leone, Surf. Sci. **204**, 455 (1988).
²²J. E. Northrup, M. C. Schabel, C. J. Karlsson, and R. I. G. Uhrberg, Phys. Rev. B **44**, 13799 (1991).
²³H. Sakama, K. Murakami, K. Nishikata, and A. Kawazu, Phys. Rev. B **50**, 14977 (1994).
²⁴J.-Z. Wang, J.-F. Jia, X. Liu, W.-D. Chen, and Q.-K. Xue, Phys. Rev. B **65**, 235303 (2002).
²⁵H. W. Yeom, T. Abukawa, Y. Takakuwa, Y. Mori, T. Shimatani, A. Kakizaki, and S. Kono, Phys. Rev. B **53**, 1948 (1996).
²⁶K. Hata, T. Kimura, S. Ozawa, and H. Shigekawa, J. Vac. Sci. Technol. A **18**, 1933 (2000).
²⁷M. Weinelt, M. Kutschera, R. Schmidt, C. Orth, T. Fauster, and M. Rohlfing, Appl. Phys. A: Mater. Sci. Process. **80**, 995 (2005).
²⁸A. A. Baski, J. Nogami, and C. F. Quate, J. Vac. Sci. Technol. A **8**, 245 (1990).
²⁹M. Weinelt, M. Kutschera, T. Fauster, and M. Rohlfing, Phys. Rev. Lett. **92**, 126801 (2004).
³⁰S. Tanaka, T. Ichibayashi, and K. Tanimura, Phys. Rev. B **79**, 155313 (2009).
³¹M. McEllistrem, G. Haase, D. Chen, and R. J. Hamers, Phys. Rev. Lett. **70**, 2471 (1993).
³²S. Chandola, J. R. Power, T. Farrell, P. Weightman, and J. F. McGilp, Appl. Surf. Sci. **123-124**, 233 (1998).
³³W. S. Fann, R. Storz, and J. Bokor, Phys. Rev. B **44**, 10980 (1991).
³⁴M. Aeschlimann, C. A. Schmuttenmaer, H. E. Elasyed-Ali, R. J. D. Miller, J. Cao, Y. Cao, and D. A. Mantell, J. Chem. Phys. **102**, 8606 (1995).
³⁵W. Mönch, *Semiconductor Surfaces and Interfaces*, 3rd ed. (Springer-Verlag, Berlin, Heidelberg, 2001).

- ³⁶T. Dekorsy, T. Pfeifer, W. Kütt, and H. Kurz, *Phys. Rev. B* **47**, 3842 (1993).
- ³⁷W. Widdra, D. Bröcker, T. Gießel, I. V. Hertel, W. Krüger, A. Lierp, F. Noack, V. Petrov, D. Pop, P. M. Schmidt, R. Weber, I. Will, and B. Winter, *Surf. Sci.* **543**, 87 (2003).
- ³⁸D. Lim and R. Haight, *J. Vac. Sci. Technol. A* **23**, 1698 (2005).
- ³⁹D. Bröcker, T. Gießel, and W. Widdra, *Chem. Phys.* **299**, 247 (2004).
- ⁴⁰S. Tokudomi, J. Azuma, K. Takahashi, and M. Kamada, *J. Phys. Soc. Jpn.* **77**, 014711 (2008).
- ⁴¹J. P. Long, B. S. Itchkawitz, and M. N. Kabler, *J. Opt. Soc. Am. B* **13**, 201 (1996).
- ⁴²D. M. Riffe, X. Y. Wang, M. C. Downer, D. L. Fisher, T. Tajima, J. L. Erskine, and R. M. More, *J. Opt. Soc. Am. B* **10**, 1424 (1993).